Contributed Papers from Materials Science and Technology 2019 (MS&T19)
September 29–October 3, 2019, Oregon Convention Center, Portland, Oregon, USA

DOI 10.7449/2019/MST_2019_356_363

SELECTIVE LASER MELTING OF Ti/SiC NANOCOMPOSITE COATING TOWARDS ENHANCED SURFACE PERFORMANCE OF Ti64

Xing Zhang[1], Bo Mao[1], Rebecca Histed[1], Mohamed Trabia[2], Brendan O'Toole[2], Richard Jennings[2], Pouya Shojaei[2], Yiliang Liao[1]

[1] Department of Mechanical Engineering, University of Nevada, Reno, Reno, Nevada, 89557 USA
[2] Department of Mechanical Engineering, University of Nevada, Las Vegas, Las Vegas, Nevada, 89154 USA

Keywords: Metal matrix nanocomposites; Selective Laser melting; Ti6Al4V

Abstract

Ti and its alloys have gained extensive applications in aerospace, marine and biomedical fields, owing to their desired properties such as high specific strength, good corrosion resistance, and excellent biocompatibility. In some applications where Ti alloys are subjected to sliding motion, the friction and wear performance is of specific importance. In recent years, metal matrix nanocomposite reinforced with nano-ceramic particles has shown great potential in improving material strength, and reducing wear and fiction. In this study, Ti/SiC nanocomposite layer was produced on Ti-6Al-4V (Ti64) substrate by laser melting. The as-fabricated nanocomposite coating exhibited a maximum surface hardness of ~700HV, which is twice as high as that of the commercial Ti64. Microstructure characterization was carried out with focus on grain size, elemental distribution and phase constituents. Moreover, the dry scratch tests showed that the wear and coefficient of friction were both significantly reduced by producing nanocomposite coating on Ti64 substrate.

Introduction

Titanium (Ti) and its alloys have gained extensive applications in aerospace, automobile, marine and biomedical fields, owing to their desired properties such as high specific strength, good corrosion resistance [1]. Dispersion of reinforced nano-ceramic particles into Ti-matrix to produce Ti-based metal matrix nanocomposites (MMNCs) can further improve the strength, high temperature stability, wear and fatigue resistance [2]. However, the incorporation of brittle ceramic reinforcements may greatly decrease the ductility and toughness of the composite material. In certain applications, the operation life of components often depends on their surface properties. Therefore, surface coating of structural components using MMNCs is desirable due to the combination of excellent surface properties and desirable ductility and toughness of the interior bulk material.

In recent years, several surface modification techniques, such as friction stir welding [3], plasma spraying [4], and thermal spraying [5], has been employed to produce MMNC coatings. Among various techniques, selective laser melting (SLM), as a newly developed additive manufacture technique, has demonstrated its promising potential in manufacturing composite material [6] and functional gradient material [7], owing to its flexibility in feedstock and layer-by-layer nature. During SLM processing of MMNCs, a layer of mixed powder (usually micro-scale powder mixing with a few amount of nano-scale particles) is firstly spread on a substrate plate. A high-energy laser beam is then applied to melt the powder layer. By repeating the powder deposition and laser scanning process, the multilayer constructions can be achieved.

In this study, Ti-based MMNC coating reinforced with 5 wt.% nano-SiC was successfully fabricated on Ti6Al4V (Ti64) substrate by SLM of a single layer. Microstructure characterization was conducted with focus on grain size, elemental distribution and phase constituents. The surface strengthening effect induced by MMNC coating was analyzed. The tribological performance of coated Ti64 was examined. The impact resistance under different impact velocity was evaluated by measuring the crater depth and diameter.

Experiments

Materials and SLM Process

Pure titanium powder with an average size of 45 μm and SiC powder with an average size of 40 nm were used as the starting material. The Ti powder was mixed with 5 wt.% SiC nanoparticle using ball milling for 4 h without protection atmosphere. The ball-to-powder ratio was 5:1, the rotation speed was 200 rpm, and 1 ml ethanol was used as a process control agent. The mixed powder with a layer thickness of 200 μm was preset on a commercial Ti64 plate. The SLM experiments were carried out using a IPG 500W fiber laser in continuous laser mode and a wavelength of 1070 nm. The laser beam size was adjusted to 200 μm, the scanning speed was fixed at 20 mm/s, and the laser power was chosen at two levels - 150 and 200 W. For a comparison, SLM experiment of pure Ti powder without nano-SiC was also carried out. The sample groups used in this study are listed in Table I.

Table I. Sample groups with different powder compositions and laser powers

Sample number	Powder composition	Laser power
I	Ti	200W
II	Ti + 5 wt.% SiC	150W
III	Ti + 5 wt.% SiC	200W

Characterization

The as-processed samples were cross-sectioned, polished and etched with Kroll's reagent for 15 s. The revealed microstructure were characterized using optical microscopy (OM) and scanning electron microscopy (SEM). The chemical and phase compositions were identified by energy dispersive X-ray spectroscopy (EDS) and X-ray diffraction (XRD).

Mechanical Properties

The Vickers hardness tests were conducted at a 500 load and a 10 s holding time. The tribological tests were performed using a ball-on-plate configuration. The ball with a diameter of 6.35 mm was made of E52100 steel with a Vickers hardness value of 746 VHN. The testing was performed at a normal load of 20 N, a reciprocating speed of 5 mm/s, and a sliding distance of 1 m. The coefficient of friction (COF) was recorded in each test. The wear rate was calculated based on the dimension of wear track. The worn surface morphologies of different samples were characterized by SEM and EDS. The impact test was carried out using a two-stage light gas gun with impact velocity varying from ~3700 to ~ 5400 km/s. The impact resistance was evaluated by measuring the depth and diameter of the crater generated during impact experiment.

Results and Discussion

Constitutional Phases

The typical XRD patterns of SLM-processed samples obtained within a range of 2θ = 20°-80° are shown in Fig. 1. The diffraction peaks for coating without SiC (sample I) indicates the as-fabricated layer consists of an α/ α' Ti as a major phase. By adding nano-SiC into the matrix, the diffraction peaks corresponding to Ti_5Si_3 and TiC phases are clearly identified in the MMNC coating fabricated by SLM with a low laser power of 150 W (sample II). Further increasing the laser power to 200 W (sample III) leads to a significant decrease of Ti_5Si_3 phase. Moreover, a few amount of retained β-Ti are found in both samples II and III.

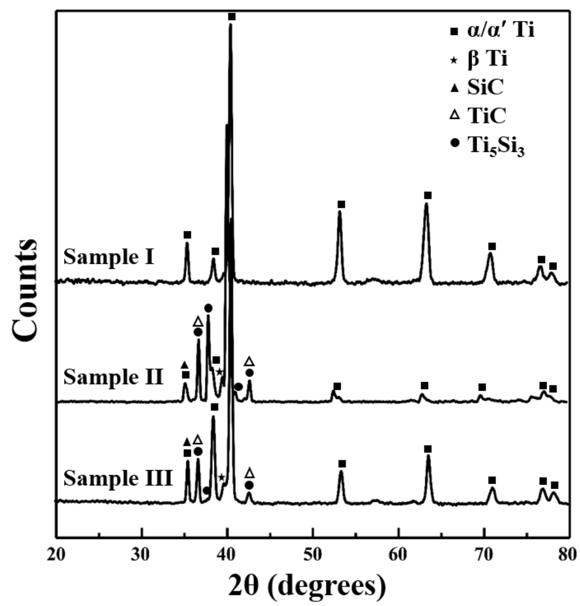

Figure 1. XRD patterns of samples I, II and III.

During SLM process, the chemical reaction between Ti and SiC are thermodynamically possible due to the negative change in Gibbs free energy, resulting in the in-situ formation of Ti_5Si_3 and TiC by:

$$Ti(l) + SiC(s) = TiC(s) + Si(s) \quad \Delta G^0 = -136.9 + 0.0095T,$$

$$5/3Ti(l) + Si(s) = 1/3\ Ti_5Si_3(s) \quad \Delta G^0 = -220.4 + 0.0265T.$$

The symbols "l" and "s" indicates liquid and solid state, respectively. As shown in the equations, the above reactions tends to occur at temperature between the melting point of Ti (1941 K) and SiC (3003 K). It is reasonable to consider that applying a low laser power of 150 W, the temperature of the molten pool rises up to a proper range where Ti_5Si_3 are massively formed. On the other hand, applying a high laser power may lead to the overheat of the mixed powder and the melting of SiC, which facilitates the formation of Ti_3SiC_2 [8]. As a result, diffraction peaks of Ti_5Si_3 phase is significantly decreased when employ a high laser power of 200 W.

Microstructure Evolution

Fig. 2 illustrates the influence of SiC addition and laser power on the microstructure evolution of SLM-processed samples. For SLM processing pure Ti powder without nano-SiC (Fig. 2a), the as-fabricated coating shows a typical microstructure of dominated α' martensite within the prior β grains. The columnar β grains have a width of 10-40 μm while much finer α' martensite forms a basketweave structure. Similar results have been observed in many other research [9], which has been attributed to the ultrafast cooling rate (>410 °C/s) during SLM process.

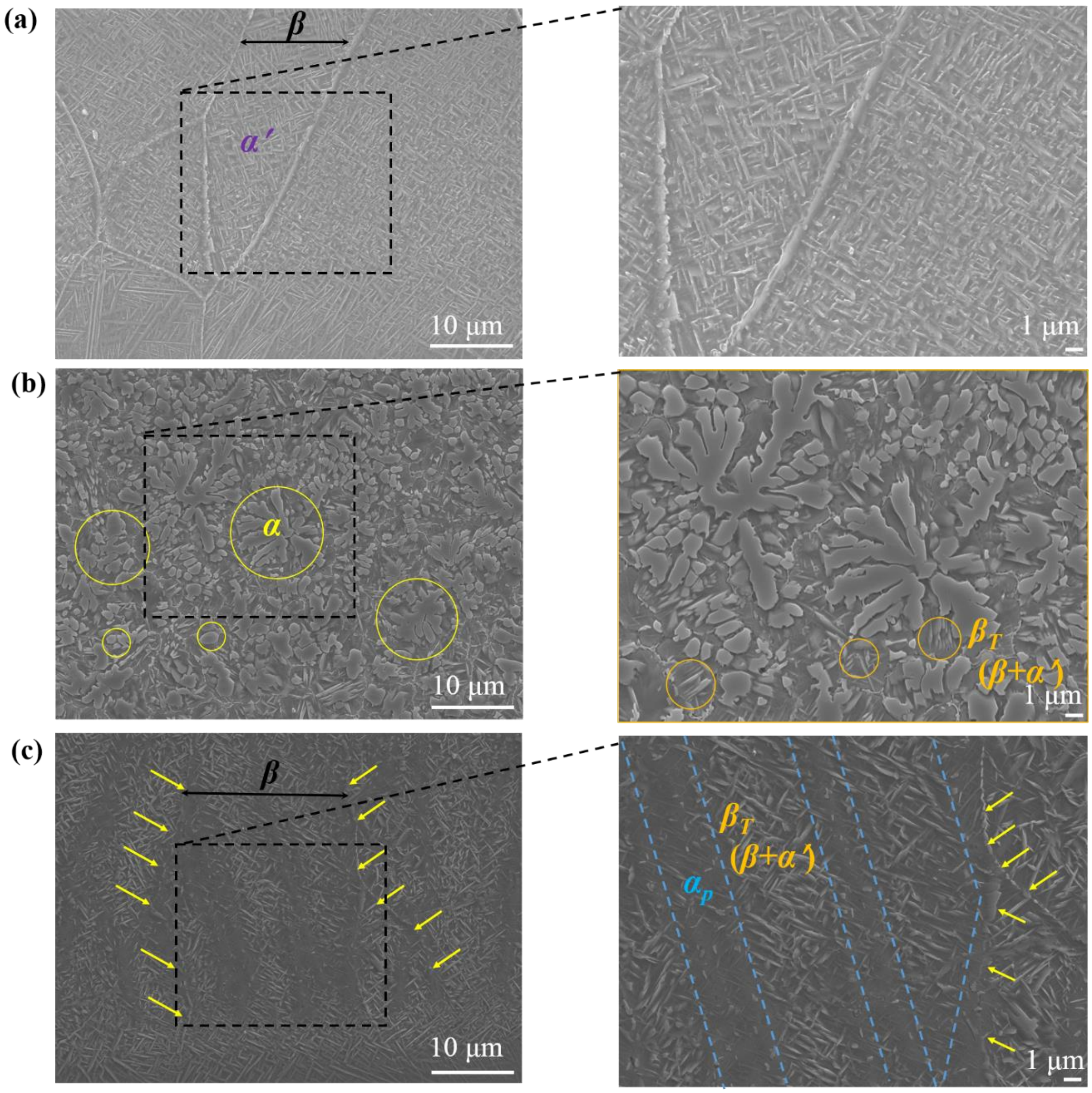

Figure. 2 SEM images of microstructure of cross-sectioned samples (a) I, (b) II, and (c) III.

By adding SiC nanoparticles into the matrix, the as-built layers present different microstructure as compared to the coating without SiC. Given a low laser power of 150 W (Fig. 2b), the MMNC coating consists of globular and dendrite grains surrounded by small equiaxed grains, forming a typical bi-modal structure [10]. The formation of equiaxed grains is majorly attributed to the presence of nano-SiC as nucleation barrier for β-Ti during the solidification process. In addition, the incorporation of nano-SiC into the matrix can decrease the cooling rate during SLM process by reducing the thermal conductivity of the composite material [11], which may also contribute to the formation of equiaxed grains. As the temperature further reduces to the β transus temperature, α'martensite is formed within the equiaxed grains. As for the globular and dendrite grains, the EDS analysis results prove a major composition of Ti (>90 wt.%). Moreover, the dendrite morphology (six-fold) and absence of acicular grains indicates that the Ti-rich phase is directly solidified to primary α-Ti instead of forming β-Ti first. It is reasonable to deduce that α-Ti was grown from the Ti_5Si_3 phase, owing to the same crystal system and small mismatch between α-Ti and Ti_5Si_3 [12].

Given a high laser power of 200 W (Fig. 2c), the MMNC coating consists of prior β grains with similar grain size of sample I. However, many sub-columnar grains with a width of 2-5 μm are observed. Those subgrains consists of α plates (α_p) and transformed β grains with α'martensite inside (β_T), forming a bi-lamellar structure [13]. As compared to the microstructure of sample II, the disappear of equiaxed grains is associated with the melting of SiC under a high laser power. In addition, the diminish of globular and dendrite α-Ti may be induced by the significant decrease of Ti_5Si_3. Furthermore, the bi-lamellar structure consisted of similar-sized α_p and β_T grains can be related to the reduced cooling rate and more released Si as a β stabilizer.

Mechanical Properties

Fig. 3 shows the average hardness measured on the surface of SLM-processed samples. It is found that the hardness values of all samples are increased as compared to the substrate of 337 VHN. The surface hardness value of sample I without SiC reinforcement is 466 VHN, similar as reported in [14], which is caused by the formation of dominated α' martensite. By adding nano-SiC, the hardness values of as-built layer further increases to 700 and 580 VHN at laser powers of 150 and 200 W, respectively. The highest hardness obtained at a laser power of 150 W is related to the formation of α' martensite, grain refinement, and dispersion strengthening induced by SiC, TiC and Ti_5Si_3. Increasing the laser power may overheat the powder layer and melt nano-SiC, which weakens the grain refinement and dispersion strengthening effects induced by SiC and Ti_5Si_3. Consequently, the hardness of MMNC coating presents a lower hardness at a higher laser power.

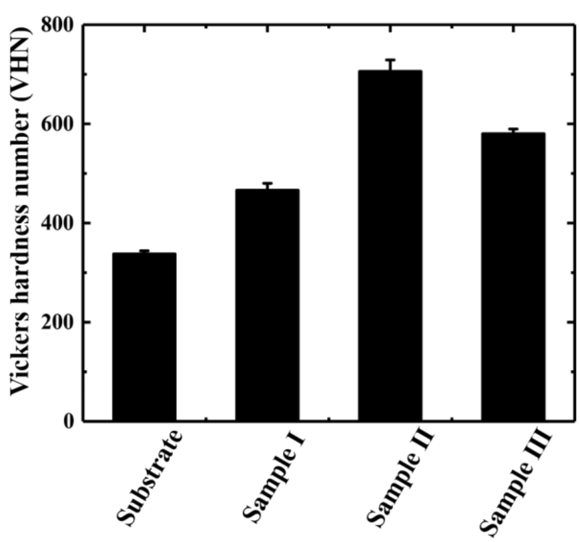

Figure. 3. Surface hardness of substrate and samples I, II and III.

Fig. 4 illustrates the effects of MMNC coating on COF and wear rate. It can be seen that the unprocessed substrate and coating without nano-SiC (sample I) show similar COF of ~0.42, while the MMNC coatings have a lower COF of ~0.38. Moreover, the MMNC coatings show significant improvement of wear rate as compared to both substrate and coating without SiC. For example, the wear rate of MMNC coating fabricated at a laser power of 150 W sharply decreased to 9×10^{-5} $mm^3/N\cdot m$, demonstrating 78.5% decrease compared to the unprocessed substrate of 42×10^{-5} $mm^3/N\cdot m$. Such reductions of COF and wear rate are essential due to the significant surface strengthening effect by MMNC layer.

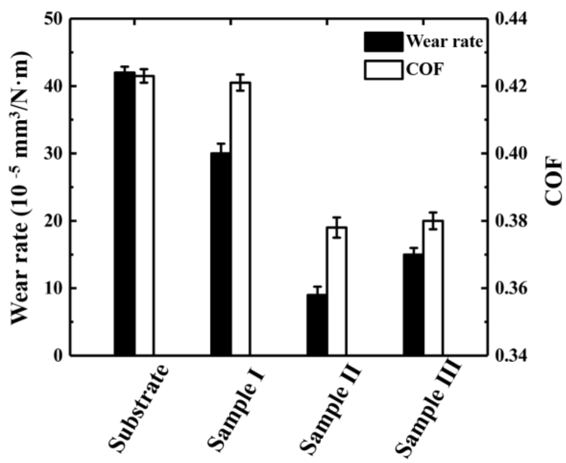

Figure. 4. COF and wear rate of substrate and samples I, II and III.

Fig. 5a shows the surface morphologies of unprocessed substrate and sample III after impact tests. The impact resistance under various impact velocities was evaluated by measuring the depth and diameter of the crater, as depicted in Fig 5b. It is found that compared to the unprocessed substrate, sample III exhibits erratic change in the crater diameter while an obvious reduction in crater depth, indicating that the impact resistance of Ti64 can be improved by producing a thin Ti/SiC MMNC layer on the surface. It is worth noting that SLM is essentially designed for layer-by-layer construction, therefore, using the SLM process to produce thick multi-layer MMNC on the substrate surface may further improve the bulk properties.

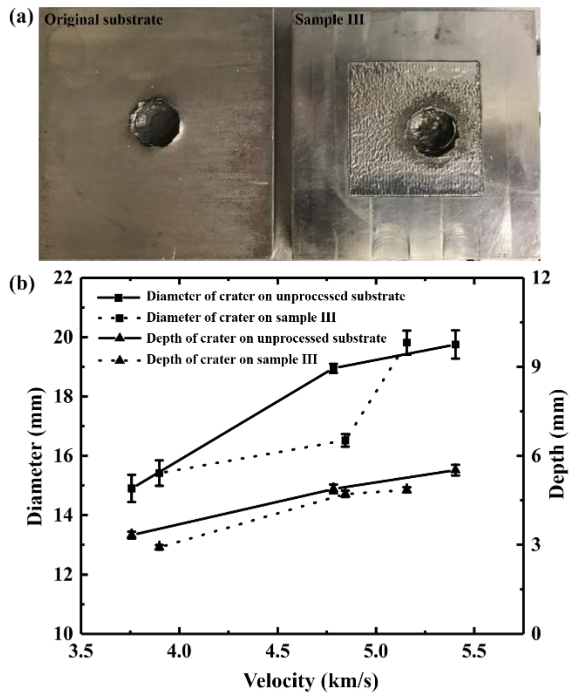

Figure.5. The comparison between

Conclusions

In this study, the SLM process was employed to fabricate Ti/SiC MMNC coating on Ti64 substrate. Grain refinement and dispersion strenthening were obtained within the MMNC layer, owing to the retained SiC and in-situ formation of TiC/Ti_5Si_3. As compared to the unprocessed substrate, the surface hardness of MMNC coated samples was maximally increased by 109% from 337 HVN to 705 HVN. The MMNC coating also led to a lower COF of 0.378 and significantly reduced the wear rate by 78.5%. It is also demonstrated that the MMNC layer has beneficial effects on bulk properties such as the impact resistance. The formation of the refined grains of Ti-matrix combined with the reinforcing particles including SiC, TiC and Ti_5Si_3 contributed to the enhancement of mechanical properties.

References

1. H. Attar, et al., "Effect of Powder Particle Shape on the Properties of In Situ Ti–TiB Composite Materials Produced by Selective Laser Melting," *Journal of Materials Science & Technology* 31, 1001-1005 (2015).
2. D. Gu, et al., "Nanocrystalline TiC reinforced Ti matrix bulk-form nanocomposites by Selective Laser Melting (SLM): Densification, growth mechanism and wear behavior," *Composites Science and Technology* 71, 1612-1620 (2011).
3. B. Zahmatkesh and M. Enayati, "A novel approach for development of surface nanocomposite by friction stir processing," *Materials Science and Engineering: A* 527, 6734-6740 (2010).
4. F. S. Alvar, et al., "Al 2 O 3-TiB 2 nanocomposite coating deposition on Titanium by Air Plasma Spraying," *Materials Today: Proceedings* 5, 15739-15743 (2018).

5. J. A. Gan and C. C. Berndt, "Nanocomposite coatings: thermal spray processing, microstructure and performance," *International Materials Reviews* 60, 195-244 (2015).
6. Y. Hu, et al., "Laser deposition-additive manufacturing of TiB-Ti composites with novel three-dimensional quasi-continuous network microstructure: Effects on strengthening and toughening," *Composites Part B: Engineering* 133, 91-100 (2018).
7. I. Shishkovsky, et al., "Graded layered titanium composite structures with TiB 2 inclusions fabricated by selective laser melting," *Composite Structures* 169, 90-96 (2017).
8. P. Krakhmalev and I. Yadroitsev, "Microstructure and properties of intermetallic composite coatings fabricated by selective laser melting of Ti–SiC powder mixtures," *Intermetallics* 46, 147-155 (2014).
9. S. Liu and Y. C. Shin, "Additive manufacturing of Ti6Al4V alloy: A review," *Materials & Design* 164, 107552 (2019).
10. R. Nalla, et al., "Influence of microstructure on high-cycle fatigue of Ti-6Al-4V: bimodal vs. lamellar structures," *Metallurgical and Materials Transactions A* 33, 899-918 (2002).
11. C. Ma, et al., "Nanoparticle-induced unusual melting and solidification behaviours of metals," *Nature communications* 8, 14178 (2017).
12. N. Li, et al., "Microstructure and Mechanical Properties of Ti6Al4V Alloy Modified and Reinforced by In Situ Ti5Si3/Ti Composite Ribbon Inoculants," *Metals* 7, 267 (2017).
13. G. Schroeder, et al., "Fatigue crack propagation in titanium alloys with lamellar and bi-lamellar microstructures," *Materials Science and Engineering: A* 319, 602-606 (2001).
14. F. Bartolomeu, et al., "Wear behavior of Ti6Al4V biomedical alloys processed by selective laser melting, hot pressing and conventional casting," *Transactions of Nonferrous Metals Society of China* 27, 829-838 (2017).